

Meshfree and efficient modelling of swimming cells

Meurig T. Gallagher* & David J. Smith†

School of Mathematics, University of Birmingham, Edgbaston, Birmingham,
B15 2TT, UK

Abstract

Locomotion in Stokes flow is an intensively-studied problem because it describes important biological phenomena such as the motility of many sperm, bacteria, algae and protozoa. Numerical computations can be challenging due to the presence of moving boundaries and complex geometries; methods which combine ease-of-implementation and computational efficiency are therefore needed. A recently-proposed method to discretise the regularised stokeslet boundary integral equation without the need for a connected ‘mesh’ is applied to the inertialess locomotion problem in Stokes flow. The mathematical formulation and key aspects of the computational implementation in Matlab®/GNU Octave are described, followed by numerical experiments with biflagellate algae and multiple uniflagellate sperm swimming between no-slip surfaces, for which both swimming trajectories and flow fields are calculated. These computational experiments required minutes of time on modest hardware; all code is provided in a github repository.

1 Introduction

Inertialess locomotion in Stokes flow describes the motility of many types of sperm, bacteria, algae and protozoa. This topic has received extensive attention from mathematical modellers, starting with the classic work of Taylor [1] and continuing to the present day [2, 3, 4]. Numerical methods are generally required to model finite amplitude motions, wall effects and swimmer-swimmer interactions. A range of numerical approaches exist, with perhaps the most extensively-studied being those based on singular, or regularized singular solutions of the Stokes flow equations, specifically resistive force theory [5], slender body theory [6], boundary integral methods [7] and regularized stokeslet methods [8, 9]. These techniques remove the need to mesh the volume of fluid, requiring only the solution of integral equations formulated on the surface of the swimming body/bodies and lines such as cilia and flagella, reducing both the cost of meshing/remeshing a continually moving domain, and the number of degrees of freedom of the resulting linear system.

As reviewed recently [10], regularized stokeslet methods have the further advantage of removing the need to evaluate weakly-singular surface integrals, and enabling slender bodies such as cilia and flagella to be treated as immersed one-dimensional curves. The original, and most widely-used, implementation of the method of regularized stokeslets of Cortez [8] has the further advantage of removing the need to generate a true *mesh*, i.e. a description of the surfaces involved in terms of connected surface elements, as is required by boundary element methods.

*M.T.Gallagher@bham.ac.uk

†D.J.Smith@bham.ac.uk

Instead it is sufficient to generate a set of points approximating the surfaces and lines of the problem geometry. A disadvantage of the original approach requires many more degrees of freedom than boundary integral methods.

To improve on the computational efficiency of the regularized stokeslet method while retaining most of its simplicity of implementation, we recently [10] proposed a method involving taking a coarser discretisation for the unknown traction than that used for numerical quadrature of the kernel, enabled by the use of nearest-neighbour discretisation. The method proved significantly more accurate for significantly lower computational cost, potentially enabling more complex and realistic problems to be investigated with given computational resources.

In this article we describe the application of the nearest-neighbour regularized stokeslet method to inertialess locomotion, in particular focusing on unflagellate pushers modelling human sperm and a model biflagellate. In section 2 we will briefly review the mathematical definition of the inertialess free-swimming problem in the boundary integral formulation. In section 3 we implement the nearest-neighbour discretisation of the free-swimming problem with a single swimmer in an unbounded fluid, and the tracking of cell trajectories through the solution of an initial-value problem. The discretisation is then generalised in section 4 to incorporate rigid boundaries and multiple swimming cells. Finally, in section 5 we present the results of numerical experiments with unflagellate and biflagellate swimmers, and in section 6 we discuss the method and its potential practical application. Key aspects of the implementation in Matlab[®]/GNU Octave are given, and a `github` repository is provided with the full code necessary to generate the results in the report.

2 The free-swimming problem

The dynamics of a Newtonian fluid at very low Reynolds numbers, associated with locomotion of cells, is described by the Stokes flow equations. The dimensionless form of the equations is,

$$-\nabla p + \nabla^2 \mathbf{u} = 0, \quad \nabla \cdot \mathbf{u} = 0, \quad (1)$$

augmented with the no-slip, no-penetration boundary condition $\mathbf{u}(\mathbf{X}) = \dot{\mathbf{X}}$ for boundary points \mathbf{X} , where overdot denotes time-derivative. Initially we will consider a single swimmer in an unbounded fluid which is stationary at infinity. Two classical problems in Stokes flow are the *resistance problem* – which involves calculating the force and moment on a rigid body made to translate and rotate in stationary fluid, and the *mobility problem* – which involves calculating the rigid body motion due to an imposed force and moment.

The free-swimming problem in Stokes flow is a variant of the mobility problem. Rather than – or perhaps in addition to – the body being driven by imposed forces, it translates and rotates as a result of changing its shape. In this section we will briefly review this problem, which has been solved numerically in many previous studies, and introduce our notation.

As usual for the regularized stokeslet method, the fluid velocity u_j at location \mathbf{x} (suppressing time-dependence) is given by a surface integral over the surface ∂D of the swimmer,

$$-\frac{1}{8\pi} \iint_{\partial D} S_{ij}^e(\mathbf{x}, \mathbf{X}) f_j(\mathbf{X}) dS_{\mathbf{X}} \approx u_i(\mathbf{x}). \quad (2)$$

The regularisation error associated with equation (2) has been discussed previously [8] and will not be reviewed here. In this paper we will treat the approximation as exact. The surface of the body will undergo motions that may be described by a model formulated in a body frame – for example a frame in which the head of the cell does not move. If the body frame coordinates are $\boldsymbol{\xi}$, and the body frame is described by the matrix of basis vectors (equivalently a rotation

matrix) $\mathbf{B} = (\mathbf{b}^{(1)}|\mathbf{b}^{(2)}|\mathbf{b}^{(3)})$ and origin \mathbf{x}_0 then the laboratory frame coordinates and velocities are,

$$\mathbf{x} = \mathbf{x}_0 + \mathbf{B} \cdot \boldsymbol{\xi}, \quad (3)$$

$$\dot{\mathbf{x}} = \dot{\mathbf{x}}_0 + \dot{\mathbf{B}} \cdot \boldsymbol{\xi} + \mathbf{B} \cdot \dot{\boldsymbol{\xi}}. \quad (4)$$

Denoting the rigid body velocity and angular velocity of the frame by \mathbf{U} and $\boldsymbol{\Omega}$ respective, we then have,

$$\mathbf{x} = \mathbf{x}_0 + \mathbf{B} \cdot \boldsymbol{\xi}, \quad (5)$$

$$\dot{\mathbf{x}} = \mathbf{U} + \boldsymbol{\Omega} \times (\mathbf{x} - \mathbf{x}_0) + \mathbf{B} \cdot \dot{\boldsymbol{\xi}}. \quad (6)$$

Applying the condition $\mathbf{u}(\mathbf{x}) = \dot{\mathbf{x}}$ on ∂D in equation (2) yields the regularized stokeslet boundary integral equation,

$$-\frac{1}{8\pi} \iint_{\partial D} S_{ij}^\epsilon(\mathbf{x}, \mathbf{X}) f_j(\mathbf{X}) dS_{\mathbf{X}} = \dot{x}_i, \quad \text{all } \mathbf{x} \in \partial D, \quad (7)$$

where it is understood that repeated indices (such as j in the above) are summed over, and unrepeated indices (such as i in the above) range over $\{1, 2, 3\}$.

If at time t , the body frame origin \mathbf{x}_0 and orientation \mathbf{B} are known, and a model is given for the swimmer shape $\boldsymbol{\xi}$ and motion $\dot{\boldsymbol{\xi}}$ in the body frame, then the unknowns of the problem are the surface traction $\mathbf{f}(\mathbf{X})$ for $\mathbf{X} \in \partial D$, the translational velocity \mathbf{U} and angular velocity $\boldsymbol{\Omega}$. The problem is closed by augmenting equation (7) with the force and moment balance equations; for the present case we will work with the assumption that the inertia and moment of inertia of the swimmer are negligible. The full problem is then given by,

$$\begin{aligned} -U_i - \epsilon_{ijk} \Omega_j (x - x_{0k}) - \frac{1}{8\pi} \iint_{\partial D} S_{ij}^\epsilon(\mathbf{x}, \mathbf{X}) f_j(\mathbf{X}) dS_{\mathbf{X}}, &= B_{ij} \dot{\xi}_j \quad \text{all } \mathbf{x} \in \partial D, \\ \iint_{\partial D} f_i(\mathbf{X}) dS_{\mathbf{X}} &= 0, \\ \iint_{\partial D} \epsilon_{ikj} X_j f_j(\mathbf{X}) dS_{\mathbf{X}} &= 0, \end{aligned} \quad (8)$$

where ϵ_{ijk} is the Levi-Civita symbol.

Numerical discretisation of the problem (8) will in general involve $3N$ unknowns for the scalar components of the traction \mathbf{f} , three unknowns for the components of the translational velocity \mathbf{U} and three unknowns for the components of the angular velocity $\boldsymbol{\Omega}$, totalling $3N + 6$ scalar unknowns in total. Through numerical collocation, problem (8) can be formulated as $3N + 6$ linear equations. In the next section we will describe a nearest-neighbour regularized stokeslet discretisation of this problem.

3 Nearest-neighbour discretisation

3.1 A single swimmer in an unbounded fluid

The discretisation of the regularized stokeslet method is discussed in detail in [10]; in brief we suggest that a good balance of ease-of-implementation and numerical efficiency can be achieved by discretising the integrals via a quadrature rule, using a finer discretisations for the rapidly-varying regularised stokeslet and a coarser discretisation for the more slowly-varying traction. A simple way to achieve this is through nearest-neighbour interpolation of the traction. The

resulting method contains the original and extensively-used method of Cortez and colleagues [8] as the special case in which the discretisations are equal.

Replacing the integrals in problem (8) with numerical quadrature yields the discrete problem,

$$\begin{aligned}
-U_i - \epsilon_{ij\ell}\Omega_j(x_k[m] - x_{0k}) - \frac{1}{8\pi} \sum_{q=1}^Q S_{ij}^\epsilon(\mathbf{x}[m], \mathbf{X}[q]) f_j(\mathbf{X}[q]) dS(\mathbf{X}[q]) &= B_{ij} \dot{\xi}_j[m], \\
&\text{for } m = 1, \dots, N, \\
\sum_{q=1}^Q f_i(\mathbf{X}[q]) dS(\mathbf{X}[q]) &= 0, \\
\sum_{q=1}^Q \epsilon_{ikj} X_k[q] f_j(\mathbf{X}[q]) dS(\mathbf{X}[q]) &= 0,
\end{aligned} \tag{9}$$

where $dS(\mathbf{X}[q])$ denotes the quadrature weight associated with the local surface metric.

Take the coarse traction discretisation as $\{\mathbf{x}[1], \dots, \mathbf{x}[N]\}$ and the finer quadrature discretisation as $\{\mathbf{X}[1], \dots, \mathbf{X}[Q]\}$, and define the $Q \times N$ nearest-neighbour matrix as,

$$\nu[q, n] = \begin{cases} 1 & \text{if } n = \underset{\hat{n}=1, \dots, N}{\operatorname{argmin}} |\mathbf{x}[\hat{n}] - \mathbf{X}[q]|, \\ 0 & \text{otherwise,} \end{cases} \tag{10}$$

Define $g_i[n] := -f_i(\mathbf{x}[n])$. Then nearest-neighbour interpolation of the traction corresponds to $-f_i(\mathbf{X}[q]) dS(\mathbf{X}[q]) \approx \sum_{n=1}^N \nu[q, n] g_i[n] dS(\mathbf{x}[n])$; applying this interpolation to problem (9) yields,

$$\begin{aligned}
\frac{1}{8\pi} \sum_{n=1}^N g_j[n] \sum_{q=1}^Q S_{ij}^\epsilon(\mathbf{x}[m], \mathbf{X}[q]) dS(\mathbf{X}[q]) \nu[q, n] - U_i - \epsilon_{ijk}\Omega_j(x_k[m] - x_{0k}) &= B_{ij} \dot{\xi}_j[m], \quad \text{for } m = 1, \dots, N, \\
\sum_{n=1}^N g_j[n] dS(\mathbf{x}[n]) \sum_{q=1}^Q \delta_{ij} \nu[q, n] &= 0, \\
\sum_{n=1}^N g_j[n] dS(\mathbf{x}[n]) \sum_{q=1}^Q \epsilon_{ikj} X_k[q] \nu[q, n] &= 0.
\end{aligned} \tag{11}$$

Computationally, problem (11) corresponds to $3N + 3 + 3$ linear equations in $3N + 3 + 3$ scalar unknowns ($F_j[n] := g_j[n] dS(\mathbf{x}[n])$ for $n = 1, \dots, N$, followed by U_j and Ω_j). These equations

can be expressed in block form as,

$$\begin{pmatrix} A_{11}^S & A_{12}^S & A_{13}^S & A_1^U & A_1^\Omega \\ A_{21}^S & A_{22}^S & A_{23}^S & A_2^U & A_2^\Omega \\ A_{31}^S & A_{32}^S & A_{33}^S & A_3^U & A_3^\Omega \\ A_1^F & A_2^F & A_3^F & & \\ A_1^M & A_2^M & A_3^M & & \end{pmatrix} \begin{pmatrix} F_1[1] \\ \vdots \\ F_1[N] \\ F_2[1] \\ \vdots \\ F_2[N] \\ F_3[1] \\ \vdots \\ F_3[N] \\ \mathbf{U} \\ \mathbf{\Omega} \end{pmatrix} = \begin{pmatrix} B_{1j}\dot{\xi}_j[1] \\ \vdots \\ B_{1j}\dot{\xi}_j[N] \\ B_{2j}\dot{\xi}_j[1] \\ \vdots \\ B_{2j}\dot{\xi}_j[N] \\ B_{3j}\dot{\xi}_j[1] \\ \vdots \\ B_{3j}\dot{\xi}_j[N] \\ \mathbf{0} \\ \mathbf{0} \end{pmatrix}, \quad (12)$$

where the blocks have entries given by,

$$\begin{aligned} A_{ij}^S\{m, n\} &= \frac{1}{8\pi} \sum_{q=1}^Q S_{ij}(\mathbf{x}[m], \mathbf{X}[q])\nu[q, n] & \text{for } m, n = 1, \dots, N, \\ A_i^U\{m, j\} &= -\delta_{ij} & \text{for } m = 1, \dots, N, \\ A_i^\Omega\{m, j\} &= -\epsilon_{ijk}(x_k[m] - x_{0k}) & \text{for } m = 1, \dots, N, \\ A_j^F\{i, n\} &= \delta_{ij} \sum_{q=1}^Q \nu[q, n] & \text{for } n = 1, \dots, N, \\ A_j^M\{i, n\} &= \epsilon_{ikj} X_k \sum_{q=1}^Q \nu[q, n] & \text{for } n = 1, \dots, N, \end{aligned} \quad (13)$$

and the velocity \mathbf{U} and angular velocity $\mathbf{\Omega}$ are expressed as 3×1 column vectors.

3.2 Computing swimmer trajectories via an initial-value problem

The position and orientation of a swimmer can be expressed as a position vector and a frame of basis vectors $\mathbf{b}^{(j)}$. Given $\mathbf{b}^{(1)}, \mathbf{b}^{(2)}$, we then have $\mathbf{b}^{(3)} = \mathbf{b}^{(1)} \times \mathbf{b}^{(2)}$ so it is sufficient to formulate the problem in terms of two basis vectors only, or six scalar degrees of freedom. Of course, this formulation still contains redundant information – three Euler angles constrain precisely the body frame, however the basis vector approach is very straightforward to implement.

Noting that

$$\begin{aligned} \dot{\mathbf{x}}_0 &= \mathbf{U}(\mathbf{x}_0, \mathbf{b}^{(1)}, \mathbf{b}^{(2)}, t), \\ \dot{\mathbf{b}}^{(j)} &= \mathbf{\Omega}(\mathbf{x}_0, \mathbf{b}^{(1)}, \mathbf{b}^{(2)}, t) \times \mathbf{b}^{(j)}, \quad j = 1, 2, \end{aligned} \quad (14)$$

we may then formulate the calculation of trajectories as a system of 9 ordinary differential equations, where evaluation of the functions $\mathbf{U}(\mathbf{x}_0, \mathbf{b}^{(1)}, \mathbf{b}^{(2)}, t)$ and $\mathbf{\Omega}(\mathbf{x}_0, \mathbf{b}^{(1)}, \mathbf{b}^{(2)}, t)$ involves solving the swimming problem (8), for example via the discretisation (11). The ‘outer’ problem (14) can be solved using built-in functions such as `ode45` in Matlab[®] or `lsode` in GNU Octave.

For practical purposes, when using a built-in initial value problem solver such as `ode45`, the tractions $f_i(\mathbf{X})$, required to compute the rate of energy dissipation and the flow field, may not

be automatically available. To record this information, we may introduce the variable $H_i(\mathbf{X}, t)$, defined by,

$$\begin{aligned} \dot{H}_i(\mathbf{x}, t) &= f_i(\mathbf{x}, t), \quad \mathbf{x} \in \partial D, \\ H_i(\mathbf{x}, 0) &= 0. \end{aligned} \quad (15)$$

Augmenting the swimming problem (14) with equations (15) then yields an approximation to the force distribution available external to `ode45` by numerically differentiating $H_i(\mathbf{x}, t)$ with respect to time.

4 Generalisation: boundaries and multiple swimmers

4.1 Boundaries and fixed obstacles

Mammalian sperm usually migrate and fertilise within a thin film of viscous fluid between opposed surfaces, and are typically imaged between a microscope slide and coverslip. Therefore it is important to take boundary effects into account in fluid dynamic simulations. The ‘blakelet’ and its regularized counterpart found by Ainley and colleagues (see also recent work by Cortez) is an elegant and efficient way to model a single infinite plane boundary; certain other geometrically simple situations possess similar fundamental solutions. However, it is important for full generality to take into account more complex boundary, and perhaps also fixed obstacles, present in the flow.

Representing the boundary by B , the swimming problem becomes,

$$\begin{aligned} -U_i - \epsilon_{ijk}\Omega_j(x_k - x_{0k}) - \frac{1}{8\pi} \iint_{\partial D \cup B} S_{ij}^\epsilon(\mathbf{x}, \mathbf{X}) f_j(\mathbf{X}) dS_{\mathbf{X}} &= B_{ij} \dot{\xi}_j, \quad \text{all } \mathbf{x} \in \partial D, \\ -\frac{1}{8\pi} \iint_{\partial D \cup B} S_{ij}^\epsilon(\mathbf{x}, \mathbf{X}) f_j(\mathbf{X}) dS_{\mathbf{X}} &= \dot{x}_i, \quad \text{all } \mathbf{x} \in B, \\ \iint_{\partial D} f_i(\mathbf{X}) dS_{\mathbf{X}} &= 0, \\ \iint_{\partial D} \epsilon_{ijk} X_j f_k(\mathbf{X}) dS_{\mathbf{X}} &= 0. \end{aligned} \quad (16)$$

Numerically, we may represent the swimmer by the force points $\{\mathbf{x}[1], \dots, \mathbf{x}[N_s]\}$ and quadrature points $\{\mathbf{X}[1], \dots, \mathbf{X}[Q_s]\}$; the boundary is then discretised by the force points $\{\mathbf{x}[N_s + 1], \dots, \mathbf{x}[N_s + N_b]\}$ and quadrature points $\{\mathbf{X}[N_s + 1], \dots, \mathbf{X}[N_s + Q_s]\}$. Nearest neighbour discretisation then leads to a system of the form,

$$\begin{pmatrix} A_{11}^S & A_{12}^S & A_{13}^S & A_1^U & A_1^\Omega \\ A_{21}^S & A_{22}^S & A_{23}^S & A_2^U & A_2^\Omega \\ A_{31}^S & A_{32}^S & A_{33}^S & A_3^U & A_3^\Omega \\ A_1^F & A_2^F & A_3^F \\ A_1^M & A_2^M & A_3^M \end{pmatrix} \begin{pmatrix} F_1 \\ F_2 \\ F_3 \\ \mathbf{U} \\ \mathbf{\Omega} \end{pmatrix} = \begin{pmatrix} V_1 \\ V_2 \\ V_3 \\ \mathbf{0} \\ \mathbf{0} \end{pmatrix}, \quad (17)$$

where the blocks have entries given by,

$$\begin{aligned}
A_{ij}^S\{m, n\} &= \frac{1}{8\pi} \sum_{q=1}^Q S_{ij}(\mathbf{x}[m], \mathbf{X}[q]) \nu[q, n] \quad \text{for } m, n = 1, \dots, N, \\
A_i^U\{m, j\} &= \begin{cases} -\delta_{ij} & \text{for } m = 1, \dots, N, \\ 0 & \text{for } m = N_s + 1, \dots, N_s + N_q, \end{cases} \\
A_i^\Omega\{m, j\} &= \begin{cases} -\epsilon_{ijk}(x_k[m] - x_{0k}) & \text{for } m = 1, \dots, N_s, \\ 0 & \text{for } m = 1, \dots, N_s + N_q, \end{cases} \\
A_j^F\{i, n\} &= \begin{cases} \delta_{ij} \sum_{q=1}^Q \nu[q, n] & \text{for } n = 1, \dots, N_s, \\ 0 & \text{for } n = N_s + 1, \dots, N_s + N_q, \end{cases} \\
A_j^M\{i, n\} &= \begin{cases} \epsilon_{ikj} X_k \sum_{q=1}^Q \nu[q, n] & \text{for } n = 1, \dots, N_s, \\ 0 & \text{for } n = N_s + 1, \dots, N_s + N_q, \end{cases}
\end{aligned} \tag{18}$$

the symbols F_j denote $(N_s + N_b) \times 1$ vectors of scalar unknowns $F_j[1], \dots, F_j[N_s + N_b]$, and the right hand sides are given by,

$$V_i[n] = \begin{cases} B_{ij} \dot{\xi}_j[n], & \text{for } n = 1, \dots, N_s, \\ 0, & \text{for } n = N_s + 1, \dots, N_s + N_b. \end{cases} \tag{19}$$

4.2 Multiple swimmers

The last situation we will consider is where there are multiple swimmers — which do not necessarily have equally-sized discretisations — as well as a boundary. The numerical discretisation is somewhat more complicated, and so we modify our notation in an attempt to make the implementation more interpretable. Suppose that we now have N_{sw} swimmers, described by collocation points with i th components $x_i^{(1)}[\cdot], \dots, x_i^{(N_{sw})}[\cdot]$, their translational and angular velocities being denoted $U_i^{(1)}, \dots, U_i^{(N_{sw})}$ and $\Omega_i^{(1)}, \dots, \Omega_i^{(N_{sw})}$; the boundary points will be denoted by the array $x_i^{(b)}[\cdot]$. The discretisation will follow the ordering convention,

$$\mathbf{x} = \begin{pmatrix} \mathbf{x}_1\{\cdot\} \\ \mathbf{x}_2\{\cdot\} \\ \mathbf{x}_3\{\cdot\} \end{pmatrix}, \tag{20}$$

where

$$\mathbf{x}_i\{\cdot\} = \begin{pmatrix} x_i^{(1)}[\cdot] \\ \vdots \\ x_i^{(N_{sw})}[\cdot] \\ x_i^{(b)}[\cdot] \end{pmatrix}, \quad (21)$$

which is inherited by the right hand side velocities and the force discretisation. If the number of force points associated with swimmer r is $N_s(r)$, and the number of force points associated with the boundary is N_b , then the number of vector force unknowns is $N_f = \sum_{r=1}^{N_{sw}} N_s(r) + N_b$. The size of \mathbf{x} is then $3N_f$ and the total number of scalar degrees of freedom in the system is $3N_f + 6N_{sw}$. We will define the index $i(r)$ to be to location of the r th swimmer in the \mathbf{x}_i vector, with $i(1) = 1$ and $i(r) = \sum_{s=1}^{r-1} N_s(s)$ for $1 < r \leq N_{sw}$.

The quadrature points may be denoted $\mathbf{X}[1], \dots, \mathbf{X}[Q]$ as previously; the stokeslet matrix is then constructed as,

$$A_{ij}^S\{\alpha, \beta\} = \frac{1}{8\pi} \sum_{q=1}^Q S_{ij}(\mathbf{x}_i[\alpha], \mathbf{X}[q])\nu[q, \beta], \quad \text{for } \alpha, \beta = 1, \dots, N_f. \quad (22)$$

To construct the remaining blocks, we introduce the notation $\mathbf{1}^{(n)}$ to be the column vector of length n with every entry equal to 1 and $\mathbf{0}^{(m \times n)}$ to be the $m \times n$ matrix of zeros. We also define the $N_f \times N_{sw}$ matrices,

$$\tilde{\mathbf{x}}_i\{\cdot, \cdot\} = \begin{pmatrix} x_i^{(1)}[\cdot] - x_{0i}^{(1)} \\ \vdots \\ x_i^{(N_{sw})}[\cdot] - x_{0i}^{(N_{sw})} \\ \mathbf{0}^{(N_b \times N_{sw})} \end{pmatrix}. \quad (23)$$

Then,

$$A^U = I_3 \otimes \begin{pmatrix} -\mathbf{1}^{(N_s(1))} & & & \\ & \ddots & & \\ & & & -\mathbf{1}^{(N_s(N_{sw}))} \\ & & \mathbf{0}^{(N_b \times N_{sw})} & \end{pmatrix}, \quad (24)$$

with \otimes denoting the Kronecker product, and

$$A^\Omega = \begin{pmatrix} & -\tilde{x}_3\{\cdot, \cdot\} & \tilde{x}_2\{\cdot, \cdot\} & \\ \tilde{x}_3\{\cdot, \cdot\} & & -\tilde{x}_1\{\cdot, \cdot\} & \\ -\tilde{x}_2\{\cdot, \cdot\} & \tilde{x}_1\{\cdot, \cdot\} & & \end{pmatrix}. \quad (25)$$

Recalling that $\nu[\cdot, \cdot]$ denotes the nearest-neighbour matrix, we define the $N_s(r) \times 1$ column vectors,

$$\begin{aligned} \lambda^{(r)}[\cdot] &= \sum_{q=1}^Q \nu[q, i(r) : i(r+1) - 1], \\ \chi_j^{(r)}[\cdot] &= \sum_{q=1}^Q X_j(q) \nu[q, i(r) : i(r+1) - 1], \end{aligned} \quad (26)$$

and the $N_{sw} \times N_f$ matrices,

$$\tilde{\chi}_j\{\cdot, \cdot\} = \begin{pmatrix} \chi_j^{(1)T}[\cdot] & & & \\ & \ddots & & \\ & & \chi_j^{(N_{sw})T}[\cdot] & \\ & & & \mathbf{0}^{(N_{sw} \times N_b)} \end{pmatrix}. \quad (27)$$

Then the $3N_{sw} \times 3N_f$ blocks A^F and A^M are,

$$A^F = I_3 \otimes \begin{pmatrix} \lambda^{(1)T}[\cdot] & & & \\ & \ddots & & \\ & & \lambda^{(N_{sw})T}[\cdot] & \\ & & & \mathbf{0}^{(N_{sw} \times N_b)} \end{pmatrix},$$

$$A^M = \begin{pmatrix} & -\tilde{\chi}_3 & \tilde{\chi}_2 & \\ \tilde{\chi}_3 & & -\tilde{\chi}_1 & \\ -\tilde{\chi}_2 & \tilde{\chi}_1 & & \end{pmatrix}. \quad (28)$$

Finally, denoting the orientation matrix of the r th swimmer by $B_{ij}^{(r)}$ and its body frame waveform as $\xi_j^{(r)}$, the terms of the right hand side take the form,

$$V_i = \begin{pmatrix} V_i^{(1)}[\cdot] \\ \vdots \\ V_i^{(N_{sw})}[\cdot] \\ \mathbf{0}^{(N_{sw} \times 1)} \end{pmatrix}, \quad (29)$$

where

$$V_i^{(r)}[n] = B_{ij}^{(r)} \dot{\xi}_j^{(r)}[n]. \quad (30)$$

Now that we have defined A_{ij}^S , A^U , A^Ω , A^F , A^M and V_i , the $3(N_f + 2) \times 3(N_f + 2)$ linear system is of the form given by equation (17).

5 Results

5.1 Biflagellate in an infinite fluid

We will first apply the algorithm in section 3.1 to model a biflagellate, superficially similar to various marine algae, swimming in an unbounded fluid. The beat pattern of the cell (figure 1(a)) is taken from a ciliate *Paramecium* beat pattern via the procedure of J.R. Blake (see [11]) – rather than a genuine biflagellate species such as *Chlamydomonas Nivalis* but it provides a sufficiently representative test case for the computational algorithm.

The two flagella are synchronised; for the force discretisation, 40 points are used to discretise each flagellum, and 96 points are used for the cell body, totalling 176 vector degrees of freedom (figure 1(a)). For the quadrature discretisation, 100 points are used for each flagellum, and 600 points for the cell body, giving a total of 700 quadrature points (figure 1(c)).

Results showing the displacement of the swimming cell are shown in figure 1(e), and the flow field at three points of the beat in figure 1(b), 1(d) and 1(f). The latter calculation can be carried out in a ‘post-processing’ step from the computed swimmer position, orientation and force distribution. While the figures show a 2D projection, the computation is fully three-dimensional, and the instantaneous flow field on any (finite) subset of \mathbb{R}^3 can be computed. The computation and creation of figure 1 required 29.5 s on a modest notebook computer (2011 Lenovo Thinkpad X220; Intel(R) Core(TM) i5-2520M CPU @ 2.50GHz; 8GB 1333 MHz DDR3 RAM).

5.2 Sperm between two opposed surfaces

We now turn our attention to the more general problem of section 4.2 involving multiple swimming cells and boundaries. The computational domain contains two no-slip square surfaces with sides of length $6L$, separated by a distance $0.4L$, where L is the flagellar length (for human sperm typically $L \approx 45 \mu\text{m}$). The flagellar movement is based on the classic planar ‘activated’ beat of Dresdner & Katz [12]; the sperm head (cell body) is a scalene ellipsoid. Figure 2(a) and 2(c) show the beat pattern via the force and quadrature discretisations respectively. The force discretisation consists of 126 points per cell and 480 points for the boundary, totalling 3330 scalar degrees of freedom for a simulation with five cells. The quadrature discretisation consists of 700 points per swimmer and 1920 points for the boundary, totalling 5420 quadrature points.

The computation shown in figure 2 involves tracking five cells each with slightly perturbed beat cycle and head morphology parameters, swimming mid-way between the no-slip boundaries described above, for six beat cycles. Figure 2(e) shows the cell trajectories, and figures 2(b), 2(d) and 2(f) shows the cell positions, orientations and surrounding flow fields at three distinct time points. The panels show one quarter of the area covered by the plane boundaries.

While the computation was more intensive than that described in the previous section, it was still easily within reach of the same notebook computer, requiring about 900 seconds of walltime.

6 Discussion

This report has described an extension of the nearest-neighbour regularized stokeslet method [10] to enable the simulation of multiple force- and moment-free cells swimming in a bounded domain. Cell trajectory calculations were achieved by casting the task as an initial-value problem; by integrating the force at each step it was additionally possible to store the evolving force distribution to enable post-calculation of the velocity field. The method was assessed on two problems of a type which may be of interest in the biological fluid mechanics community: swimming of a biflagellate in an unbounded domain, and motility of multiple human sperm between two no-slip surfaces.

This pilot study suggests that the method is relatively efficient, requiring minutes to solve the problems described above, without specialist computational hardware. It may therefore be valuable for high-throughput analysis of experimental data, or (perhaps with adaptations to deal efficiently with long-range interactions) suspensions of relatively large numbers of swimmers. While the construction of the matrices is somewhat tedious, the underlying concept of the method — a coarse/fine discretisation of the boundary integral equations to address the fact that the force distribution varies more slowly than the kernel — should ensure that the method is comprehensible and extensible by non-specialists. Crucially, no true ‘mesh’ generation (i.e. with connectivity tables) is required to simulate a new swimmer of interest. We hope that these properties of ease-of-use, extensibility and efficiency make the method appealing to potential

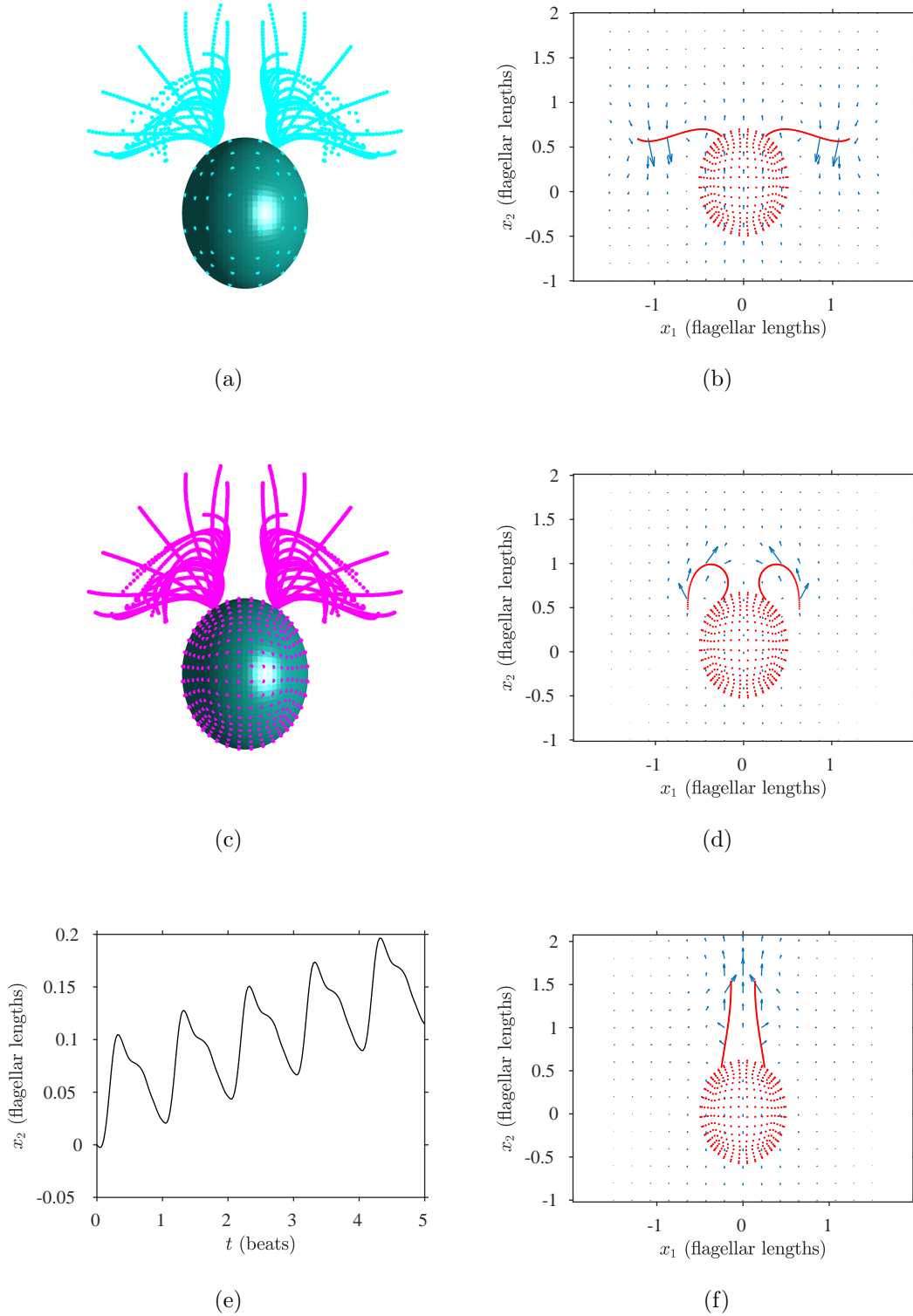


Figure 1: Computational results for a free-swimming model biflagellate in an unbounded fluid, implemented with the script `GenerateSwimmingFigureChlamy.m` (a,c) Model biflagellate showing beat pattern, visualised via (a) force discretisation, (c) quadrature discretisation. (b,d,f) computed flow fields at (b) $t = 2\pi/3$, (d) $t = 4\pi/3$ and (f) $t = 2\pi$ (three points during the beat cycle). (e) x_2 coordinate of free-swimming cell over five beat cycles, where positive x_2 is the overall swimming direction.

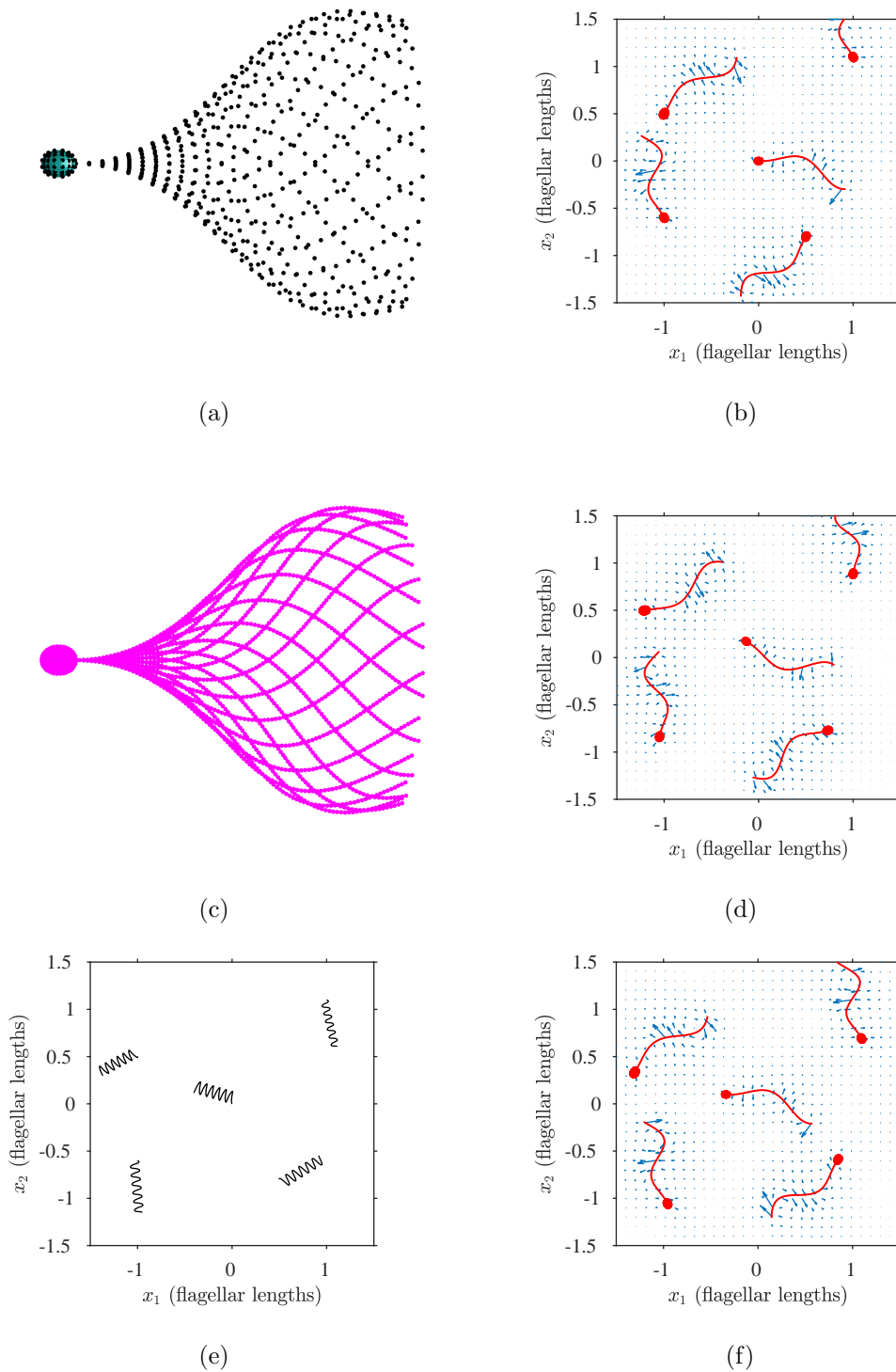


Figure 2: Computational results for a group of free-swimming model sperm swimming between midway between two opposed no-slip surfaces separated by 0.4 flagellar lengths, implemented with the script `GenerateSwimmingFigureSperm.m` (a,c) Model sperm showing beat pattern of Dresdner & Katz, visualised via (a) force discretisation, (c) quadrature discretisation. (b,d,f) computed cell positions (with 5 randomly-perturbed beat cycles and head dimensions), and flow fields at (b) $t = 0$, (d) $t = 2.5$ cycles and (f) $t = 5$ cycles. (e) Trajectories of free-swimming cells over six beat cycles.

users, and in support of this aim we provide all Matlab[®] code used to generate this report in the repository github.com/djsmithbham/nearestStokesletSwimmers.

7 Acknowledgements

This work was supported by Engineering and Physical Sciences Research Council award EP/N021096/1.

References

- [1] G.I. Taylor. Analysis of the swimming of microscopic organisms. *Proc. R. Soc. Lond. A.*, 209:447–461, 1951.
- [2] E.E. Keaveny, S.W. Walker, and M.J. Shelley. Optimization of chiral structures for microscale propulsion. *Nano Lett.*, 13(2):531–537, 2013.
- [3] J. Simons, L. Fauci, and R. Cortez. A fully three-dimensional model of the interaction of driven elastic filaments in a Stokes flow with applications to sperm motility. *J. Biomech.*, 48(9):1639–1651, 2015.
- [4] K. Ishimoto, H. Gadêlha, E.A. Gaffney, D.J. Smith, and J. Kirkman-Brown. Coarse-graining the fluid flow around a human sperm. *Phys. Rev. Lett.*, 118(12):124501, 2017.
- [5] J. Gray and G.J. Hancock. The propulsion of sea urchin spermatozoa. *J. Exp. Biol.*, 32:802–814, 1955.
- [6] J.J.L. Higdon. A hydrodynamic analysis of flagellar propulsion. *J. Fluid Mech.*, 90:685–711, 1979.
- [7] N. Phan-Thien, T. Tran-Cong, and M. Ramia. A boundary-element analysis of flagellar propulsion. *J. Fluid Mech.*, 185:533–549, 1987.
- [8] R. Cortez, L. Fauci, and A. Medovikov. The method of regularized Stokeslets in three dimensions: Analysis, validation, and application to helical swimming. *Phys. Fluids*, 17:031504, 2005.
- [9] E.A. Gillies, R.M. Cannon, R.B. Green, and A.A. Pacey. Hydrodynamic propulsion of human sperm. *J. Fluid Mech.*, 625:445, 2009.
- [10] D.J. Smith. A nearest-neighbour discretisation of the regularized stokeslet boundary integral equation. *J. Comput. Phys.*, 358:88–102, 2018.
- [11] D.J. Smith. Biological fluid mechanics under the microscope: A tribute to John Blake. *ANZIAM J.*, In press, 2018.
- [12] R.D. Dresdner and D.F. Katz. Relationships of mammalian sperm motility and morphology to hydrodynamic aspects of cell function. *Biol. Reprod.*, 25(5):920–930, 1981.